

Concentration-Dependent Two-Dimensional Halogen-Bonded Self-Assembly of 1,3,5-Tris(4-iodophenyl)benzene Molecules at the Solid–Liquid Interface

Fabien Silly

▶ **To cite this version:**

Fabien Silly. Concentration-Dependent Two-Dimensional Halogen-Bonded Self-Assembly of 1,3,5-Tris(4-iodophenyl)benzene Molecules at the Solid–Liquid Interface. Journal of Physical Chemistry C, 2017, 121, pp.10413 - 10418. 10.1021/acs.jpcc.7b02091 . cea-01591526

HAL Id: cea-01591526

https://cea.hal.science/cea-01591526

Submitted on 21 Sep 2017

HAL is a multi-disciplinary open access archive for the deposit and dissemination of scientific research documents, whether they are published or not. The documents may come from teaching and research institutions in France or abroad, or from public or private research centers.

L'archive ouverte pluridisciplinaire **HAL**, est destinée au dépôt et à la diffusion de documents scientifiques de niveau recherche, publiés ou non, émanant des établissements d'enseignement et de recherche français ou étrangers, des laboratoires publics ou privés.

THE JOURNAL OF PHYSICAL CHEMISTRY C

Article

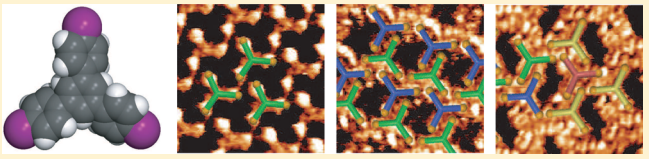
pubs.acs.org/JPCC

Concentration-Dependent Two-Dimensional Halogen-Bonded Self-Assembly of 1,3,5-Tris(4-iodophenyl)benzene Molecules at the Solid−Liquid Interface

Fabien Silly*

TITANS, SPEC, CEA, CNRS, Université Paris-Saclay, CEA Saclay 91191 Gif sur Yvette, France

ABSTRACT: The concentration-dependent self-assembly of star-shaped 1,3,5-tris(4-iodophenyl)benzene at the 1-phenyloctane/graphite interface is investigated using scanning tunneling microscopy. The molecules self-assemble into a hexagonal porous halogen-bonded nanoarchitecture at low concentration. This structure is stabilized by X_3 synthons. The molecules are oriented along the same direction in this arrangement. At higher concentration two molecular orientations are observed. The molecules then form a porous parallelogram halogen-bonded structure stabilized by X_2 synthons. The density of molecular packing is thus higher at high solution concentration. High solution concentration also leads to the appearance of domain boundary in the parallelogram structure. Iodine bonds appear to be a promising alternative to hydrogen bonds to engineer tunable organic porous structures on flat surfaces.



INTRODUCTION

Molecular self-assembly offers unique possibilities for engineering two-dimensional (2D) nanoarchitectures on metal surfaces. The internal structure of these organic structures can be tailored at the atomic scale by exploiting intermolecular interactions.[1,2] Strong directional intermolecular bindings are required to stabilize the formation of porous systems. Porous nanoarchitectures have been already produced taking advantage of intermolecular hydrogen bonding.[1,3−10] The strength,[11] the high selectivity, and the high directionality of this intermolecular binding[12−15] prevent the formation of close-packed structures. Hybrid metal−organic and organic−ionic compound interactions have recently proven to be a selective and directional interaction that can stabilize the formation of sophisticated porous hybrid 2D structures.[16−20] The halogen bond (X bond) appears to be an appealing alternative to these localized interactions to tailor molecular self-assembly at the atomic scale.[21−27] The X bond is also a selective and directional intermolecular interaction. The strength of this bond is however strongly depending of its geometry.[28]

Hydrogen-[1,3−12,14,15,29−34] as well as halogen-bonded[3,22,23,26,27,35−47] organic nanoarchitectures have been successfully engineered in vacuum but also at the solid/liquid interface. In that case the solvent nature[48−50] and molecular concentration can drastically affect the structure of the organic layer. Stepanenko et al., for example, investigated the concentration-dependent self-assembly of linear oligophenyleneethylene-based complexes at the solid/liquid interface.[51] They observed that these complexes form a 2D lamellar structure at high concentration, whereas sophisticated rhombitrihexagonal Archimedean tiling arrangements appear at low concentration. The molecular Cl ligands appear to play a key role in the molecular self-assembly through multiple C−H···Cl interactions. Hu et al. also showed that molecular concentration can drastically affect the self-assembly of molecules with halogen atoms at the solid/liquid interface.[52] Under saturated concentration they observed that some specific molecules form linear lamellae resulting from intermolecular van der Waals interactions. At lower concentration, solvent adsorbs on the surface and modifies the intermolecular interactions. Three solvent−molecule halogen and hydrogen bonds dominate the structural formation of the organic layer at low concentration. In these two examples[51,52] the molecules possess halogen atoms and alkyl chains. It is therefore not clear if the variation of solution concentration mainly influences intermolecular halogen bonding or modifies the van der Waals interactions between adjacent molecular alkyl chains. To unveil the influence of solution concentration on halogen bonding, molecules without alkyl chains have to be selected. Eder et al. showed that increasing molecular concentration can lead to the formation of a nonorganized second monolayer of 1,3,5-tris(4-iodophenyl)benzene molecules on Au(111).[53] Gatti et al. observed that solvent molecules can sometimes interact with molecules without an alkyl chain and form a 2D bicomponent structure on Au(111).[54]

In this paper the concentration-dependent self-assembly of 1,3,5-tris(4-iodophenyl)benzene molecules at the 1-phenyloctane/graphite interface is investigated. These molecules do not have alkyl chains. Three solution concentrations are studied. Scanning tunneling microscopy (STM) reveals that solution concentration can drastically influence the halogen bonding between neighboring molecules. The internal structure of the self-assembled organic layer varies with solution concentration.

Received: March 4, 2017
Revised: April 23, 2017
Published: April 27, 2017

ACS Publications © 2017 American Chemical Society

DOI: 10.1021/acs.jpcc.7b02091
J. Phys. Chem. C 2017, 121, 10413−10418

EXPERIMENTAL SECTION

Solutions of 1,3,5-tris(4-iodophenyl)benzene (90%, Aldrich) in 1-phenyloctane (Aldrich) were prepared. A droplet of the solution was then deposited on a graphite substrate. STM imaging of the samples was performed at the liquid−solid interface using a Pico-SPM (Molecular Imaging, Agilent Technology) scanning tunneling microscope. Cut Pt/Ir tips were used to obtain constant current images at room temperature with a bias voltage applied to the sample. STM images were processed and analyzed using the application FabViewer.[55]

RESULTS

The chemical structure of the 1,3,5-tris(4-iodophenyl)benzene molecule is presented in Figure 1. This 3-fold symmetry molecule is a star-shaped molecule. The molecular skeleton consists of a central benzene ring connected to three peripheral 4′-iodophenyl groups. The iodine atom separation is 1.34 nm.

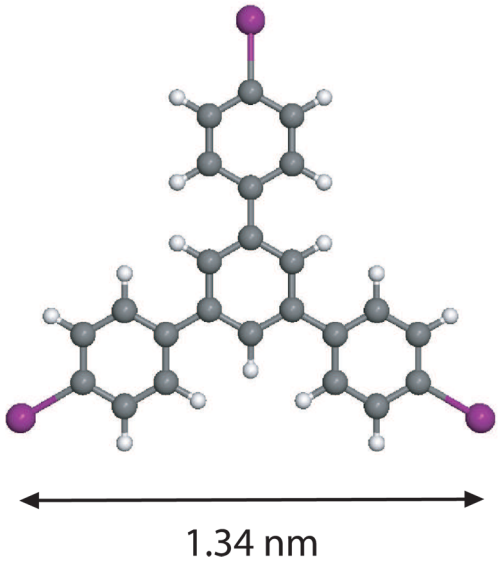


Figure 1. Scheme of 1,3,5-tris(4-iodophenyl)benzene ($C_{21}H_{15}I_3$) dimer building block. Carbon atoms are gray, iodine atoms purple, and hydrogen atoms white.

The STM image in Figure 2 shows the graphite surface after deposition of a droplet of low concentration solution (<10^{-9} mol./L) of 1,3,5-tris(4-carboxyphenyl)benzene molecules in 1-phenyloctane. Molecules self-assemble into a large-scale 2D organic nanoarchitecture. A high-resolution STM image is presented in Figure 2b. The molecular iodine atoms appear brighter in the STM image.[56] As a guide for the eyes, a molecular model has been superimposed to the STM image. The molecular carbon skeleton is represented by a green star, whereas iodine atoms appear as yellow balls. Only one molecular orientation is observed in this structure. The molecular self-assembly is porous. The structure appears to be stabilized by X_3 synthons between neighboring molecules (one X_3 synthon is highlighted by a yellow circle in Figure 2 b). The angle between I···I bonds is 120°. The network unit cell of this porous hexagonal structure is a parallelogram with 1.8 ± 0.2 nm unit cell constants and an angle of 60 ± 2° between the axes. The unit cell is represented by a dashed yellow parallelogram in Figure 2b.

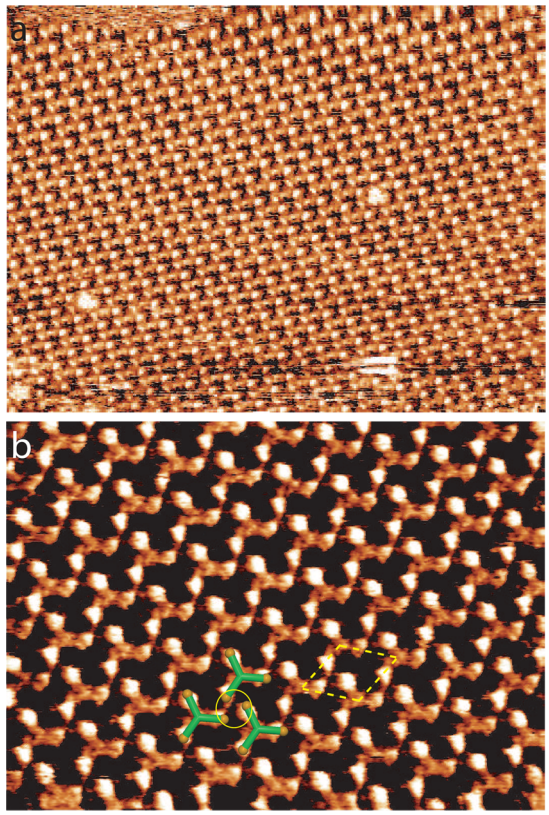


Figure 2. STM image of the 1,3,5-tris(4-iodophenyl)benzene self-assembled porous network at the 1-phenyloctane/graphite interface: (a) 40 × 30 nm^2, (b) 15 × 11 nm^2, V_s = 0.7 V, I_t = 9 pA. Molecular scheme has been superimposed to the STM image as a guide for the eyes.

The STM image in Figure 3 shows the graphite surface after deposition of a droplet of a higher concentration solution (10^{-7}

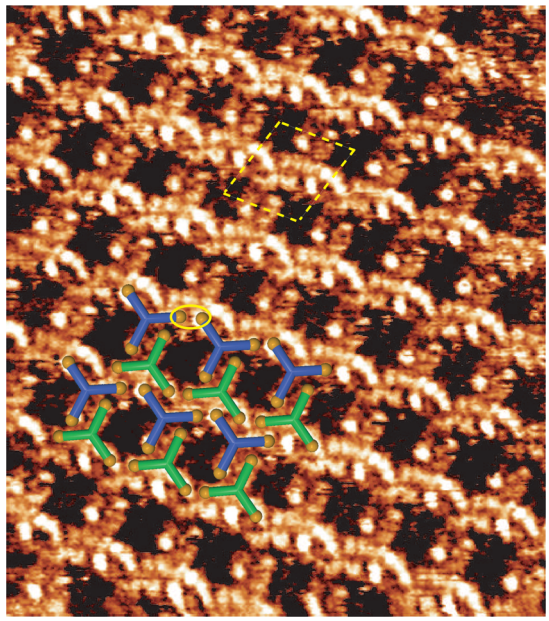


Figure 3. STM image of the 1,3,5-tris(4-iodophenyl)benzene self-assembled porous network at the 1-phenyloctane/graphite interface, 13 × 11 nm^2, V_s = 0.4 V, I_t = 13 pA. Blue and green molecular schemes have been superimposed to the STM image as a guide for the eyes.

DOI: 10.1021/acs.jpcc.7b02091
J. Phys. Chem. C 2017, 121, 10413−10418

mol./L) of 1,3,5-tris(4-carboxyphenyl)benzene molecules in 1-phenyloctane. Molecules self-assembled into a second 2D porous organic nanoarchitecture. As a guide for the eyes, molecular schemes have been superimposed to the STM image. Two molecular orientations can now be observed in the organic network. Molecular closest neighbors are rotated by 180°. The two molecular orientations are represented by molecules in blue and green colors superimposed to the STM image in Figure 3. Molecules with different orientations are arranged side-by-side and are forming dimers (a molecular dimer is composed of a blue and a green molecule). The 2D nanoarchitecture is stabilized by X_2 synthons between neighboring dimers (an X_2 synthon is highlighted by a yellow ellipse in Figure 3). The molecules with identical orientation are thus forming chains also stabilized by X_2 synthons. The angle between I···I bonds is 120°. The network unit cell of this porous structure is a parallelogram with 1.7 ± 0.2 nm and 1.9 ± 0.2 nm lattice constants and an angle of 73 ± 2° between the axes. The unit cell is represented by a dashed yellow parallelogram in Figure 3.

The STM image in Figure 4 shows the graphite surface after deposition of a droplet of a high-concentration solution (10^{-6} mol./L) of 1,3,5-tris(4-carboxyphenyl)benzene molecules in 1-phenyloctane. Molecules self-assemble into a 2D porous organic nanoarchitecture very similar to the one previously observed in Figure 3. Schemes of molecular dimers have been superimposed to the STM image in Figure 4. A molecular dimer is composed of one blue and one green molecule rotated by 180°. The large-scale STM image in Figure 4a shows that dimers are not perfectly aligned in the large-scale image of the surface. Domain boundaries are observed in the STM image. The domain boundaries are highlighted by yellow dashed lines and black arrows in Figure 4a.

A high-resolution STM image of the network domain boundary is presented in Figure 4b. As a guide for the eyes, molecular dimers of neighboring domains have been represented in different colors, i.e., blue-green colors and yellow-red colors. The molecules of neighboring domains conserve the same orientation. The internal structure of neighboring domains is identical and was described above in Figure 3. Only the local molecular arrangement at the domain boundary is different. Cavities are formed at the domain boundary. The cavity shape observed inside the organic domain is highlighted by a light blue dashed rectangle in Figure 4b, whereas the cavity shape observed at the domain boundary is highlighted by a yellow dashed rectangles. The cavity inside the domain is formed by two green and two blue molecules, whereas the cavity at the domain boundary is formed by one green, one blue, one yellow, and one red molecule, Figure 4b. The cavity shape inside the domain and at the domain boundary is chiral. The cavity models, presented in Figure 4b, reveal that the cavity at the domain boundary is the mirror-symmetry equivalent of the cavity inside the domain. This structure is chiral because of the steric arrangement of the molecules, i.e., molecular dimers are chiral. No other molecular nanoarchitectures were observed at higher solution concentration.

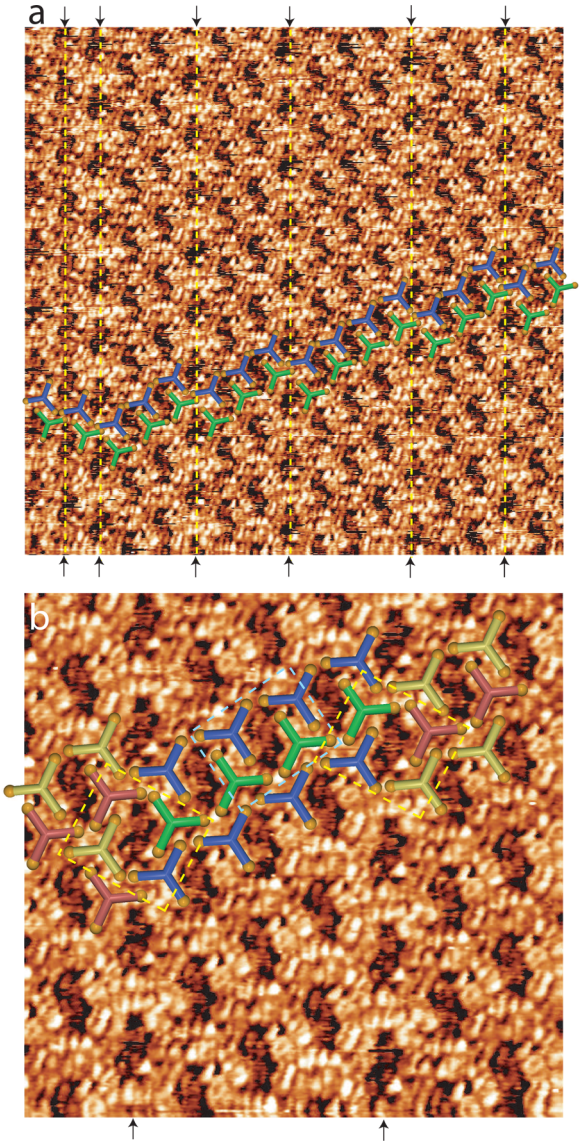


Figure 4. STM image of the 1,3,5-tris(4-iodophenyl)benzene self-assembled porous network at the 1-phenyloctane/graphite interface: (a) 40 × 30 nm^2, V_s = 0.4 V, I_t = 13 pA (dotted yellow lines highlight the domain boundary); (b) 13 × 13 nm^2. Molecular schemes (yellow, red, green, and blue) have been superimposed to the STM image as a guide for the eyes. Dotted yellow and light blue rectangles highlight the two cavity shapes observed in the organic layer. Black arrows in a and b indicate the position of the network domain boundary.

DISCUSSION

STM shows that 1,3,5-tris(4-iodophenyl)benzene molecules self-assemble into different 2D porous nanoarchitectures at the 1-phenyloctane/graphite interface. These halogen-bonded structures strongly differ from those observed when the molecules are self-assembling in vacuum on Au(111).[56] The 1,3,5-tris(4-iodophenyl)benzene self-assembly at the 1-phenyl-octaone/graphite interface appears to be strongly dependent on the solution concentration. STM reveals that at low concentration ($<10^{-9}$ mol/L) the molecules self-assemble into a hexagonal porous structure. Only one molecular orientation is observed in this nanoarchitecture. This 2D arrangement is stabilized by X_3 halogen synthons. The network density is 2.8 nm^2/mol. At a concentration of ~10^{-7} mol./L, the molecules are forming a second 2D nanoarchitecture having a parallelogram unit cell. This structure is now stabilized by X_2 halogen synthons and van der Waals interactions resulting from the side-by-side arrangement of neighboring molecules forming dimers. This increases the network density that is now 1.5 nm^2/mol. For higher concentration solution, 10^{-6} mol/L, the

DOI: 10.1021/acs.jpcc.7b02091
J. Phys. Chem. C 2017, 121, 10413−10418

molecules still self-assemble into the parallelogram structure but defects are now observed. Molecules are now not perfectly aligned on a large distance, Figure 4b. Domain boundaries are now observed. The boundary of self-assembled star-shaped molecule domains may be defective.[56,57] This is not the case here. Molecules are well ordered at the domain boundary, and no domain gap is observed. Well-aligned cavities are observed in this area. STM reveals that the cavities formed at the domain boundaries are the mirror-symmetry equivalent of the cavity formed inside the molecular domain. The STM images show that increasing the solution concentration leads thus to the formation of a higher density 2D nanoarchitecture. It should be noticed that there are no solvent molecules in the cavities of the different organic networks.[58] The density of the parallelogram nanoarchitecture is in fact 46% more dense than the hexagonal structure. High-concentration solutions lead to an increase of domain nucleation sites and therefore to the appearance of domain boundaries. The nucleation and growth dynamics of organic layer from solution-deposited organic compounds are more complex than vapor deposited compounds, since solvent/surface interactions, compound/solvent interactions, and compound/surface interactions have to be taken into consideration. Nucleation is a competition between the thermodynamic driving force (volume effects and enthalpic lowering of free energy by beneficial intermolecular interactions) and the energetic penalty associated with surface effects, i.e., creation of new surfaces. The rate of nucleation of stable domain of organic compounds is a function of the rate of deposition, surface temperature, surface properties, intermolecular interactions, and molecule−surface interactions. Nucleation rate is thus increasing with the deposition rate.[59] This means that domain nucleation is therefore increasing at higher solution concentration. As the neighboring domains are not perfectly aligned, this leads to an increasing probability of domain boundary formation at high solution concentration. New theoretical developments to model the 2D growth of organic nanoarchitectures are required to estimate the dynamics of domain boundary formation. In contrast with ref 53, no formation of a second layer of molecules was observed on a graphite surface at high solution concentration and even for saturated concentration.

Bui et al. previously showed that the strength of the halogen bond depends of the C−X···X−C binding angle.[28] For an angle of 180°, the halogen bond is similar to van der Waals interaction. In comparison, the strength of the halogen bond is stronger and similar to hydrogen bonds when the C−X···X−C angle is 120°. The 2D nanoarchitectures observed at low (Figure 2) and high concentrations (Figures 3 and 4) appear therefore to be stabilized by the strongest halogen bond, as the C−I···I−C angle is 120°.

CONCLUSION

To summarize, the influence of solution concentration on star-shaped 1,3,5-tris(4-iodophenyl)benzene self-assembly at the 1-phenyloctane/graphite interface was investigated using scanning tunneling microscopy. Molecules self-assemble into different porous halogen-bonded nanoarchitectures depending on the solution concentration. High solution concentrations also lead to the appearance of a domain boundary. These observations show that iodine···iodine bonds are promising intermolecular binding to control and tune two-dimensional molecular organization. This opens up new opportunities for engineering tailored organic nanoarchitectures having sophisticated structures.

AUTHOR INFORMATION

Corresponding Author

*E-mail: fabien.silly@cea.fr. Phone: +33(0)169088019. Fax: +33(0)169088446.

ORCID

Fabien Silly: 0000-0001-6782-9268

Notes

The author declares no competing financial interest.

ACKNOWLEDGMENTS

The research leading to these results has received funding from the European Research Council under the European Union's Seventh Framework Programme (FP7/2007-2013)/ERC grant agreement no. 259297.

REFERENCES

(1) Liang, H.; Sun, W.; Jin, X.; Li, H.; Li, J.; Hu, X.; Teo, B. K.; Wu, K. Two-Dimensional Molecular Porous Networks Formed by Trimesic Acid and 4,4′Bis(4-pyridyl)biphenyl on Au(111) through Hierarchical Hydrogen Bonds: Structural Systematics and Control of Nanopore Size and Shape. *Angew. Chem., Int. Ed.* **2011**, *50*, 7562−7566.

(2) Yang, Y.; Wang, C. Hierarchical Construction of Self-Assembled Low-Dimensional Molecular Architectures Observed by Using Scanning Tunneling Microscopy. *Chem. Soc. Rev.* **2009**, *38*, 2576.

(3) Baris, B.; Luzet, V.; Duverger, E.; Sonnet, P.; Palmino, F.; Chérioux, F. Robust and Open Tailored Supramolecular Networks Controlled by the Template Effect of a Silicon Surface. *Angew. Chem., Int. Ed.* **2011**, *50*, 4094−4098.

(4) Uemura, S.; Aono, M.; Komatsu, T.; Kunitake, M. Two-Dimensional Self-Assembled Structures of Melamine and Melem at the Aqueous Solution-Au(111) Interface. *Langmuir* **2011**, *27*, 1336−1340.

(5) Shen, C.; Cebula, I.; Brown, C.; Zhao, J.; Zharnikov, M.; Buck, M. Structure of isophthalic acid based monolayers and its relation to the initial stages of growth of metal-organic coordination layers. *Chem. Sci.* **2012**, *3*, 1858−1865.

(6) Temirov, R.; Soubatch, S.; Neucheva, O.; Lassise, A. C.; Tautz, F. S. A novel method achieving ultra-high geometrical resolution in scanning tunnelling microscopy. *New J. Phys.* **2008**, *10*, 053012.

(7) Chen, T.; Yang, W.-H.; Wang, D.; Wan, L.-J. Globally Homochiral Assembly of Two-Dimensional Molecular Networks Triggered by Co-Absorbers. *Nat. Commun.* **2013**, *4*, 1389.

(8) Silly, F.; Shaw, A. Q.; Briggs, G. A. D.; Castell, M. R. Epitaxial Ordering of a Perylenetetracarboxylic Diimide-melamine Supramolecular Network Driven by the Au(111)-(22 × $\sqrt{3}$) Reconstruction. *Appl. Phys. Lett.* **2008**, *92*, 023102.

(9) Gardener, J. A.; Shvarova, O. Y.; Briggs, G. A. D.; Castell, M. R. Intricate Hydrogen-Bonded Networks: Binary and Ternary Combinations of Uracil, PTCDI, and Melamine. *J. Phys. Chem. C* **2010**, *114*, 5859−5866.

(10) Räisänen, M. T.; Slater, A. G.; Champness, N. R.; Buck, M. Effects of pore modification on the templating of guest molecules in a 2D honeycomb network. *Chem. Sci.* **2012**, *3*, 84−92.

(11) Barth, J. V. Molecular Architectonic on Metal Surfaces. *Annu. Rev. Phys. Chem.* **2007**, *58*, 375−407.

(12) Tanioku, C.; Matsukawa, K.; Matsumoto, A. Thermochromism and Structural Change in Polydiacetylenes Including Carboxy and 4-Carboxyphenyl Groups as the Intermolecular Hydrogen Bond Linkages in the Side Chain. *ACS Appl. Mater. Interfaces* **2013**, *5*, 940−948.

(13) Mura, M.; Silly, F.; Burlakov, V.; Castell, M. R.; Briggs, G. A. D.; Kantorovich, L. N. Formation Mechanism for a Hybrid Supra-

DOI: 10.1021/acs.jpcc.7b02091
J. Phys. Chem. C 2017, 121, 10413−10418

molecular Network Involving Cooperative Interactions. *Phys. Rev. Lett.* **2012**, *108*, 176103.
(14) Priimagi, A.; Lindfors, K.; Kaivola, M.; Rochon, P. Efficient Surface-Relief Gratings in Hydrogen-Bonded Polymer-Azobenzene Complexes. *ACS Appl. Mater. Interfaces* **2009**, *1*, 1183−1189.
(15) Hieulle, J.; Silly, F. Localized Intermolecular Electronic Coupling in Two-Dimensional Self-Assembled 3,4,9,10-perylenetetracarboxylic Diimide Nanoarchitectures. *J. Mater. Chem. C* **2013**, *1*, 4536−4539.
(16) Urgel, J. I.; Écija, D.; Lyu, G.; Zhang, R.; Palma, C.-A.; Auwärter, W.; Lin, N.; Barth, J. V. Quasicrystallinity Expressed in Two-Dimensional Coordination Networks. *Nat. Chem.* **2016**, *8*, 657−662.
(17) Zhang, C.; Wang, L.; Xie, L.; Ding, Y.; Xu, W. On-Surface Dual-Response Structural Transformations of Guanine Molecules and Fe Atoms. *Chem. - Eur. J.* **2017**, *23*, 2356−2362.
(18) Sun, Q.; Cai, L.; Ma, H.; Yuan, C.; Xu, W. On-Surface Construction of a Metal-Organic Sierpiński Triangle. *Chem. Commun.* **2015**, *51*, 14164−14166.
(19) Cirera, B.; Đordević, L.; Otero, R.; Gallego, J. M.; Bonifazi, D.; Miranda, R.; Ecija, D. Dysprosium-carboxylate nanomeshes with tunable cavity size and assembly motif through ionic interactions. *Chem. Commun.* **2016**, *52*, 11227−11230.
(20) Hieulle, J.; Peyrot, D.; Jiang, Z.; Silly, F. Engineering Two-Dimensional Hybrid NaCl-Organic Coordinated Nanoarchitectures on Metal Surfaces. *Chem. Commun.* **2015**, *51*, 13162−13165.
(21) Zheng, Q.-N.; Liu, X.-H.; Chen, T.; Yan, H.-J.; Cook, T.; Wang, D.; Stang, P. J.; Wan, L.-J. Formation of Halogen Bond-Based 2D Supramolecular Assemblies by Electric Manipulation. *J. Am. Chem. Soc.* **2015**, *137*, 6128−6131.
(22) Xu, J.; Liu, X.; Ng, J. K.-P.; Lin, T.; He, C. Trimeric Supramolecular Liquid Crystals Induced by Halogen Bonds. *J. Mater. Chem.* **2006**, *16*, 3540−3545.
(23) Gao, H. Y.; Shen, Q. J.; Zhao, X. R.; Yan, X. Q.; Pang, X.; Jin, W. J. Phosphorescent Co-Crystal Assembled by 1,4-diiodotetrafluorobenzene with Carbazole Based on C-I···π Halogen Bonding. *J. Mater. Chem.* **2012**, *22*, 5336−5343.
(24) Getmanenko, Y. A.; Fonari, M.; Risko, C.; Sandhu, B.; Galán, E.; Zhu, L.; Tongwa, P.; Hwang, D. K.; Singh, S.; Wang, H.; et al. Benzo[1,2-b:6,5-b′] dithiophene(dithiazole)-4,5-dione derivatives: synthesis, electronic properties, crystal packing and charge transport. *J. Mater. Chem. C* **2013**, *1*, 1467−1481.
(25) Lafferentz, L.; Eberhardt, V.; Dri, C.; Africh, C.; Comelli, G.; Esch, F.; Hecht, S.; Grill, L. Controlling On-Surface Polymerization by Hierarchical and Substrate-Directed Growth. *Nat. Chem.* **2012**, *4*, 215−220.
(26) Metrangolo, P.; Resnati, G.; Pilati, T.; Liantonio, R.; Meyer, F. Engineering Functional Materials by Halogen Bonding. *J. Polym. Sci., Part A: Polym. Chem.* **2007**, *45*, 1−15.
(27) Meyer, F.; Dubois, P. Halogen Bonding at Work: Recent Applications in Synthetic Chemistry and Materials Science. *CrystEngComm* **2013**, *15*, 3058−3071.
(28) Bui, T. T. T.; Dahaoui, S.; Lecomte, C.; Desiraju, G. R.; Espinosa, E. The Nature of Halogen···Halogen Interactions: A Model Derived from Experimental Charge-Density Analysis. *Angew. Chem., Int. Ed.* **2009**, *48*, 3838−3841.
(29) Yagai, S. Supramolecularly Engineered Functional π-Assemblies Based on Complementary Hydrogen-Bonding Interactions. *Bull. Chem. Soc. Jpn.* **2015**, *88*, 28−58.
(30) Xu, L.; Miao, X.; Zha, B.; Deng, W. Hydrogen-Bonding-Induced Polymorphous Phase Transitions in 2D Organic Nanostructures. *Chem. - Asian J.* **2013**, *8*, 926−933.
(31) Hu, Y.; Miao, K.; Zha, B.; Xu, L.; Miao, X.; Deng, W. STM Investigation of Structural Isomers: Alkyl Chain Position Induced Self-Assembly at the Liquid/Solid Interface. *Phys. Chem. Chem. Phys.* **2016**, *18*, 624−634.
(32) Hu, Y.; Miao, K.; Peng, S.; Zha, B.; Xu, L.; Miao, X.; Deng, W. Structural transition control between dipole-dipole and hydrogen bonds induced chirality and achirality. *CrystEngComm* **2016**, *18*, 3019−3032.
(33) Silly, F. Two-Dimensional 1,3,5-Tris(4-carboxyphenyl)benzene Self-Assembly at the 1-Phenyloctane/Graphite Interface Revisited. *J. Phys. Chem. C* **2012**, *116*, 10029−10032.
(34) Sun, X.; Jonkman, H. T.; Silly, F. Tailoring Two-Dimensional PTCDA-melamine Self-Assembled Architectures at Room Temperature by Tuning Molecular Ratio. *Nanotechnology* **2010**, *21*, 165602.
(35) Shang, J.; Wang, Y.; Chen, M.; Dai, J.; Zhou, X.; Kuttner, J.; Hilt, G.; Shao, X.; Gottfried, J. M.; Wu, K. Assembling Molecular Sierpiński Triangle Fractals. *Nat. Chem.* **2015**, *7*, 389−393.
(36) Silly, F. Selecting Two-Dimensional Halogen-Halogen Bonded Self-Assembled 1,3,5-Tris(4-iodophenyl)benzene Porous Nanoarchitectures at the Solid-Liquid Interface. *J. Phys. Chem. C* **2013**, *117*, 20244−20249.
(37) Getmanenko, Y. A.; Fonari, M.; Risko, C.; Sandhu, B.; Galán, E.; Zhu, L.; Tongwa, P.; Hwang, D. K.; Singh, S.; Wang, H.; et al. Benzo[1,2-b:6,5-b′]dithiophene(dithiazole)-4,5-dione derivatives: synthesis, electronic properties, crystal packing and charge transport. *J. Mater. Chem. C* **2013**, *1*, 1467−1481.
(38) Voth, A. R.; Khuu, P.; Oishi, K.; Ho, P. S. Halogen bonds as orthogonal molecular interactions to hydrogen bonds. *Nat. Chem.* **2009**, *1*, 74−79.
(39) Lieberman, H. F.; Davey, R. J.; Newsham, D. M. T. Br···Br and Br···H Interactions in Action: Polymorphism, Hopping, and Twinning in 1,2,4,5-Tetrabromobenzene. *Chem. Mater.* **2000**, *12*, 490−494.
(40) Gutzler, R.; Fu, C.; Dadvand, A.; Hua, Y.; MacLeod, J. M.; Rosei, F.; Perepichka, D. F. Halogen Bonds in 2D Supramolecular Self-Assembly of Organic Semiconductors. *Nanoscale* **2012**, *4*, 5965−5971.
(41) DiLullo, A.; Chang, S.-H.; Baadji, N.; Clark, K.; Klöckner, J.-P.; Prosenc, M.-H.; Sanvito, S.; Wiesendanger, R.; Hoffmann, G.; Hla, S.-W. Molecular Kondo Chain. *Nano Lett.* **2012**, *12*, 3174−3179.
(42) Chung, K.-H.; Kim, H.; Jang, W. J.; Yoon, J. K.; Kahng, S.-J.; Lee, J.; Han, S. Molecular Multistate Systems Formed in Two-Dimensional Porous Networks on Ag(111). *J. Phys. Chem. C* **2013**, *117*, 302−306.
(43) Meazza, L.; Foster, J. A.; Fucke, K.; Metrangolo, P.; Resnati, G.; Steed, J. W. Halogen-bonding-triggered supramolecular gel formation. *Nat. Chem.* **2013**, *5*, 42−47.
(44) Sun, A.; Lauher, J. W.; Goroff, N. S. Preparation of Poly(diiododiacetylene), an Ordered Conjugated Polymer of Carbon and Iodine. *Science* **2006**, *312*, 1030−1034.
(45) Pigge, F. C.; Vangala, V. R.; Kapadia, P. P.; Swenson, D. C.; Rath, N. P. Hexagonal crystalline inclusion complexes of 4-iodophenoxy trimesoate. *Chem. Commun.* **2008**, 4726−4728.
(46) Metrangolo, P.; Meyer, F.; Pilati, T.; Resnati, G.; Terraneo, G. Mutual induced coordination in halogen-bonded anionic assemblies with (6,3) cation-templated topologies. *Chem. Commun.* **2008**, 1635−1637.
(47) Zha, B.; Dong, M.; Miao, X.; Peng, S.; Wu, Y.; Miao, K.; Hu, Y.; Deng, W. Cooperation and competition between halogen bonding and van der Waals forces in supramolecular engineering at the aliphatic hydrocarbon/graphite interface: position and number of bromine group effects. *Nanoscale* **2017**, *9*, 237−250.
(48) Lee, S.-L.; Chu, Y.-C.; Wu, H.-J.; Chen, C.-h. Template-Assisted Assembly: Scanning Tunneling Microscopy Study of Solvent-Dependent Adlattices of Alkyl-Derivatized Tetrathiafulvalene. *Langmuir* **2012**, *28*, 382−388.
(49) Gutzler, R.; Cardenas, L.; Rosei, F. Kinetics and thermodynamics in surface-confined molecular self-assembly. *Chem. Sci.* **2011**, *2*, 2290−2300.
(50) Shao, X.; Luo, X.; Hu, X.; Wu, K. Solvent Effect on Self-Assembled Structures of 3,8-Bis-hexadecyloxy-benzo[c]cinnoline on Highly Oriented Pyrolytic Graphite. *J. Phys. Chem. B* **2006**, *110*, 1288−1293.
(51) Stepanenko, V.; Kandanelli, R.; Uemura, S.; Würthner, F.; Fernández, G. Concentration-Dependent Rhombitrihexagonal Tiling patterns at the Liquid/Solid Interface. *Chem. Sci.* **2015**, *6*, 5853−5858.
(52) Hu, X.; Zha, B.; Wu, Y.; Miao, X.; Deng, W. Effects of the Position and Number of Bromine Substituents on the Concentration-

DOI: 10.1021/acs.jpcc.7b02091
J. Phys. Chem. C 2017, 121, 10413−10418

Mediated 2D Self-Assembly of Phenanthrene Derivatives. *Phys. Chem. Chem. Phys.* **2016**, *18*, 7208−7215.
(53) Eder, G.; Smith, E. F.; Cebula, I.; Heckl, W. M.; Beton, P. H.; Lackinger, M. Solution Preparation of Two-Dimensional Covalently Linked Networks by Polymerization of 1,3,5-Tri(4-iodophenyl)-benzene on Au(111). *ACS Nano* **2013**, *7*, 3014−3021.
(54) Gatti, R.; MacLeod, J. M.; Lipton-Duffin, J. A.; Moiseev, A. G.; Perepichka, D. F.; Rosei, F. Substrate, Molecular Structure, and Solvent Effects in 2D Self-Assembly via Hydrogen and Halogen Bonding. *J. Phys. Chem. C* **2014**, *118*, 25505−25516.
(55) Silly, F. A Robust Method For Processing Scanning Probe Microscopy Images and Determining Nanoobject Position and Dimensions. *J. Microsc.* **2009**, *236*, 211−218.
(56) Peyrot, D.; Silly, F. On-Surface Synthesis of Two-Dimensional Covalent Organic Structures versus Halogen-Bonded Self-Assembly: Competing Formation of Organic Nanoarchitectures. *ACS Nano* **2016**, *10*, 5490−5498.
(57) Silly, F. Two-Dimensional Self-Assembly of 2,4,6-Tris(4′,4″,4‴-Trimethylphenyl)-1,3,5-Triazine Star-Shaped Molecules: Nanoarchitecture Structure and Domain Boundaries. *J. Phys. Chem. C* **2014**, *118*, 11975−11979.
(58) Marie, C.; Silly, F.; Tortech, L.; Müllen, K.; Fichou, D. Tuning the Packing Density of 2D Supramolecular Self-Assemblies at the Solid-Liquid Interface Using Variable Temperature. *ACS Nano* **2010**, *4*, 1288−1292.
(59) Markov, I. V. *Crystal growth for beginners: fundamentals of nucleation, crystal growth, and epitaxy*; World Scientific: Singapore; River Edge, NJ, 1995; 01078.

DOI: 10.1021/acs.jpcc.7b02091
J. Phys. Chem. C 2017, 121, 10413−10418